Journal of Rare Cardiovascular Diseases
ISSN: 2299-3711 (Print) | e-ISSN: 2300-5505 (Online)
www.jrcd.eu

RESEARCH ARTICLE

Eco-Friendly Fabrication of Zinc Oxide Nanoparticles Enriched with Astaxanthin Extracted from Haematococcus pluvialis and Their Antioxidant and Anti-Inflammatory Potentials

Sakthivel Muthu[1], Visnu Sasithra[2], Pranav Mahender[3] and Shenbhagaraman Ramalingam[4]
[1]Department of Dermatology, Saveetha Medical College and Hospital, Saveetha Institute of Medical and Technical Sciences (SIMATS), Thandalam, Chennai-602105, Tamil Nadu, India;
[2]Department of Orthopaedics, Saveetha Medical College and Hospital, Saveetha Institute of Medical and Technical Sciences (SIMATS), Thandalam, Chennai-602105, Tamil Nadu, India;
[3]Third Year Undergraduate, Saveetha Medical College and Hospital, Saveetha Institute of Medical and Technical Sciences (SIMATS), Thandalam, Chennai-602105, Tamil Nadu, India;
[4]Department of ENT, Saveetha Medical College and Hospitals, Saveetha Institute of Medical and Technical Sciences (SIMATS), Saveetha University, Chennai-602105, India;

*Corresponding Author
Shenbhagaraman Ramalingam

Article History
Received: 09/07/2025
Revised: 23/08/2025
Accepted: 12/09/2025
Published: 30/09/2025

Abstract: Green nanotechnology has emerged as a sustainable alternative for synthesizing functional nanomaterials with biomedical relevance. This study focuses on the environmental friendly production of zinc oxide nanoparticles (ZnO NPs) using astaxanthin derived from Haematococcus pluvialis, targeting antioxidant and anti-inflammatory applications. Astaxanthin was extracted from 10 g of dried H. pluvialis biomass using acetone, producing 36.8 mg of reddish pigment. The bio-extract was employed as a reactant and capping agent in the green synthesis of ZnO NPs. UV-Vis spectroscopy was employed to screen nanoparticle formation. FTIR spectroscopy was conducted to identify active molecules responsible for stabilization. Distribution pattern of particle size was estimated using dynamic light scattering (DLS), while surface charge was analysed via zeta potential analysis. Morphological examination was performed through scanning electron microscopy (SEM). Antioxidant and anti-inflammatory properties were assessed using standard radical scavenging and protein denaturation assays. UV-Vis studies revealed an absorption peak at 360 nm, demonstrating nanoparticle synthesis. FTIR spectra indicated functional group interactions and a Zn–O bond at 581 cm^{-1}. DLS measured particle size between 85–110 nm with a zeta potential of –27.5 mV, suggesting enough stability. SEM images showed spherical particles ranging from 50–80 nm. Antioxidant activities (DPPH, H_2O_2, NO) reached up to ~80% at 100 µg/mL, while anti-inflammatory assays showed over 79% inhibition, closely aligning with standard drugs. ZnO NPs synthesized using astaxanthin exhibit potent bioactivity, underscoring their potential in therapeutic applications.

Keywords: Haematococcus pluvialis, Astaxanthin, Zinc oxide nanoparticles, Characterization, Antioxidant activity, Anti-inflammatory assay.

INTRODUCTION

In recent years, the merging of nanotechnology and natural product chemistry has led to the expansion of novel therapeutic agents with improved biological functions and reduced toxicity[1]. Zinc oxide nanoparticles (ZnO NPs) have enlarged noteworthy interest across various biomedical domains due to their inherent properties such as high surface-to-volume ratio, optical transparency, antimicrobial potential, and relative biocompatibility[2]. These nanoparticles are widely used in pharmaceuticals, cosmetics, and biomedical applications, especially drug delivery vehicles, imaging agents, and therapeutic modulators. However, the traditional physicochemical synthesis methods for ZnO NPs often comprise hazardous reagents, high energy consumption, and environmentally unfriendly byproducts, thereby necessitating the adoption of green synthesis strategies[3].

Green synthesis, which uses biological systems such as plant sources, algae, bacteria, or fungi, has developed as an eco-friendly, sustainable, and biocompatible alternative[4]. Among these biological resources, microalgae are especially promising due to their fast growth rate, ease of cultivation, and the ability to biosynthesize a wide array of bioactive compounds[5]. *Haematococcus pluvialis*, a freshwater green microalga, is particularly notable for its ability to gather high levels of astaxanthin—a red-orange xanthophyll carotenoid with exceptional antioxidant and anti-inflammatory properties [6].

Astaxanthin, a naturally occurring keto-carotenoid, is well-documented for its capability to hunt reactive oxygen species (ROS), prevent peroxidation of lipid moiety, and control key inflammatory mediators such as COX-2 and NF-κB. Its potent free radical neutralizing capacity is attributed to the presence of conjugated double bonds and hydroxyl/keto functional groups on both ends of its polyene chain [7]. However, the medical usage of astaxanthin is often hindered by its poor aqueous solubility, low stability under physiological conditions, and limited bioavailability. Integrating astaxanthin with a nanocarrier such as ZnO NPs may offer a hopeful approach to overcome these restrictions by refining stability, solubility , and targeted delivery [8].

In this context, the present study explores a green, one-pot eco-friendly approach for fabricating zinc oxide nanoparticles using astaxanthin extracted from *Haematococcus pluvialis* as both reacting agent and capping agent. The approach not only minimizes the use of harmful chemicals but also facilitates the functionalization of ZnO NPs with bioactive molecules, potentially leading to synergistic therapeutic effects. The synthesized astaxanthin-integrated ZnO NPs are systematically described using suitable techniques, including UV-Visible spectroscopy, FTIR, DLS, and electron microscopy, to confirm their structural, morphological, and functional properties. Furthermore, the biological efficacy of these nanoconjugates is evaluated through in vitro antioxidant tests like DPPH, Superoxide Anion Scavenging Activity (H_2O_2), and Nitric Oxide (NO) Scavenging Assay and anti-inflammatory assessments including inhibition of nitric oxide production in lipopolysaccharide (LPS)-stimulated macrophages. The integration of astaxanthin into ZnO nanostructures is hypothesized to not only retain but enhance the antioxidant and anti-inflammatory efficacy due to increased stability and cellular uptake.

MATERIALS AND METHODS

Materials

Zinc acetate dihydrate [$Zn(CH_3COO)_2 \cdot 2H_2O$], sodium hydroxide (NaOH), 1,1-diphenyl-2-picrylhydrazyl (DPPH), hydrogen peroxide (H_2O_2), sodium nitroprusside, sulfanilamide, N-(1-naphthyl)ethylenediamine dihydrochloride (NED), and other analytical-grade chemicals were procured from HiMedia Laboratories (India). *Haematococcus pluvialis* biomass was obtained from a certified algal culture collection. All reagents used were of analytical grade.

Extraction of Astaxanthin from *Haematococcus pluvialis*

The *Haematococcus pluvialis* biomass was harvested and dried under shade. Ten grams of powdered dry biomass was subjected to solvent extraction using acetone in a 1:20 (w/v) ratio [9]. The suspension was stirred for 4–6 hours in the dark at room temperature, followed by centrifugation at 5000 rpm for 15 minutes. The supernatant was collected, and the extraction process was repeated until the pellet lost its reddish color. The pooled extracts were concentrated using a rotary evaporator at 40°C and stored at –20°C until further use. The presence of astaxanthin was confirmed using UV–Vis and HPLC analyses.

Green Synthesis of Astaxanthin-Functionalized Zinc Oxide Nanoparticles

To form ZnO nanoparticles, 50 mL of 0.01 M zinc acetate solution was prepared and maintain at 60°C under uninterrupted stirring. A freshly prepared astaxanthin extract (10 mL) was added dropwise as a reactant and stabilizing agent[10]. The pH was altered to 10 using 0.1 M NaOH. The reaction mixture was maintained at 60°C for 2 hours, resulting in a pale yellow precipitate indicating nanoparticle formation. The suspension was chilled to 25°C and subjected to centrifugation at 10,000 rpm for 20 minutes. The pellet was rinsed thrice with distilled water and ethanol, then dehydrated at 60°C and stored for characterization and biological assays.

UV–Visible Spectroscopy

Ultraviolet–visible (UV–Vis) spectroscopy was employed to monitor the formation and optical properties of the synthesized ZnO-astaxanthin nanoparticles. The absorption spectra were acquired across the 200–800 nm wavelength range using a UV–Visible spectrophotometer. The presence of a characteristic absorption peak around 350–380 nm indicated the successful formation of zinc oxide nanoparticles due to their intrinsic surface plasmon resonance. Additionally, the spectral shift or broadening in the peak confirmed the capping and functionalization of the nanoparticles by astaxanthin extracted from *Haematococcus pluvialis*, suggesting effective integration of the bioactive compound onto the nanoparticle surface.

Fourier Transform Infrared (FTIR) Spectroscopy

FTIR analysis was carried out to detect the functional moiety responsitble for reduction and stabilization of ZnO nanoparticles by astaxanthin. The samples were recorded in the spectral range of 4000–400 cm^{-1} using an FTIR spectrophotometer. Peaks corresponding to hydroxyl (–OH), carbonyl (C=O), and C–H stretching vibrations were observed, which are typical of astaxanthin and its associated biomolecules. The shifts in peak positions compared to pure astaxanthin extract suggested strong interactions between astaxanthin and the nanoparticle surface, thereby confirming the successful capping and stabilization of ZnO nanoparticles by phytochemical constituents.

Dynamic Light Scattering (DLS) and Zeta Potential Analysis

DLS was accomplished to define the hydrodynamic diameter and particle size distribution of the ZnO-astaxanthin nanoparticles in colloidal suspension. The measurements were taken using a Zetasizer Nano ZS at room temperature. Zeta potential analysis was done to measure the surface charge and colloidal stability of the nanoparticles. A high absolute zeta potential value (either positive or negative) suggested electrostatic stabilization of the nanoparticles, which prevents aggregation and ensures stability in suspension.

Scanning Electron Microscopy (SEM)

The surface morphology and topographical features of the ZnO-astaxanthin nanoparticles were observed using scanning electron microscopy. A thin layer of the dried nanoparticle powder was positioned on a carbon-coated grid and sputter-coated with a thin layer of gold to improve conductivity. SEM images revealed the shape, size, and degree of aggregation of the nanoparticles. The particles appeared predominantly spherical or oval, with some degree of clustering, which is common in biosynthesized nanoparticles. The observed morphology further confirmed the successful synthesis and stabilization of ZnO nanoparticles using astaxanthin.

Antioxidant Assays

DPPH Free Radical Scavenging Assay

The antioxidant activity was determined using the DPPH radical scavenging method. A 0.1 mM DPPH solution in methanol was prepared. In a 96-well ELISA plate, 100 µL of DPPH reagent was added with 100 µL of 10–100 µg/mL concentrations of ZnO-astaxanthin nanoparticles[11]. The reaction mixtures were kept in the place away from the light for 30 minutes at room temperature. The OD was read at 517 nm using a microplate reader. Positive control used in this experiment was Ascorbic acid. The percentage of DPPH inhibition was estimated using the formula:

$$\%\ \boldsymbol{of\ DPPH\ Inhibition} = \frac{\boldsymbol{A\ Control - A\ Sample}}{\boldsymbol{Acontrol}} \boldsymbol{X100}$$

H_2O_2 Scavenging Assay

40 mM of hydrogen peroxide (H_2O_2) was made in phosphate-buffered saline (pH 7.4). In a 96-well plate, 100 µL of H_2O_2 reagent was mixed with 100 µL of ZnO-astaxanthin nanoparticles at various concentrations (10–100 µg/mL) [12]. After 10 minutes of incubation at 25°C, OD was recorded at 230 nm. The scavenging ability of the nanoparticles was matched to that of ascorbic acid, and the percentage of H_2O_2 scavenging activity was calculated using the following formula.

$$\%\ \boldsymbol{of\ Hydrogen\ peroxide\ scavenging} = \frac{\boldsymbol{A\ Control - A\ Sample}}{\boldsymbol{Acontrol}} \boldsymbol{X100}$$

Nitric Oxide (NO) Assay

The nitric oxide radical scavenging was calculated by adding 100 µL of 10 mM sodium nitroprusside reagent prepared using phosphate buffer (pH 7.4) with 100 µL of nanoparticle suspension at varying concentrations (10–100 µg/mL) in a 96-well plate. The mixtures were maintained at 25°C for 2 hours under light to allow NO generation. After incubation, 100 µL of the reaction mixture was added to100 µL of Griess reagent (2% phosphoric acid containing 0.1% NED and 1% sulfanilamide) and kept at 25°C for 10 minutes. The OD was measured at 540 nm. The percentage of NO inhibition was estimated as below

$$\%\ \boldsymbol{of\ NO\ inhibition} = \frac{\boldsymbol{A\ Control - A\ Sample}}{\boldsymbol{Acontrol}} \boldsymbol{X100}$$

Anti-inflammatory Activity

The anti-inflammatory effect of the produced ZnO-astaxanthin nanoparticles was assessed by means of *in vitro* protein denaturation inhibition assay and membrane stabilization assay, which simulate inflammatory conditions by evaluating the inhibition of albumin denaturation and erythrocyte membrane lysis, respectively.

Protein Denaturation Inhibition Assay

This method is based on the inhibition of heat-induced denaturation of egg albumin, mimicking the inflammatory process. Fresh hen's egg was used to prepare a 5% aqueous solution of albumin[13]. To each test tube, 1 mL of albumin solution was added to 1 mL of PBS, pH 6.3 and 1 mL of ZnO-astaxanthin nanoparticle suspension at various concentrations (10–100 µg/mL). The resulting reagent were incubated at 37°C for 20 minutes and then for 5 minutes maintained at 70°C. The solution was allowed to cool and the turbidity was determined at 660 nm using a UV–Visible spectrophotometer. The results were compared with standard drug Diclofenac sodium. The protein denaturation inhibition percentage of was determined as:

$$\%\ \boldsymbol{of\ protein\ denaturation\ \ inhibition} = \frac{\boldsymbol{A\ Control - A\ Sample}}{\boldsymbol{Acontrol}} \boldsymbol{X100}$$

Human Red Blood Cell (HRBC) Membrane Stabilization Assay

The assay evaluates the ability of nanoparticles to stabilize the human erythrocyte membrane, an indirect measure of anti-inflammatory potential. Blood sample was obtained and red blood cells (RBCs) were separated by centrifuging at 3000 rpm for 10 minutes[14]. The pellet was washed three times with isotonic saline and re-suspended as a 10% v/v RBC suspension in phosphate buffer (pH 7.4).

In each test tube, 1 mL of ZnO-astaxanthin nanoparticles (10–100 µg/mL), 1 mL of 10mM phosphate buffer containing 0.25% NaCl, and 0.5 mL of 10% RBC suspension were added. The tubes were maintained at 37°C for 30 minutes, then centrifuged for 10 minutes at 3000 rpm. The OD of the supernatant was measured at 560 nm. Diclofenac sodium served as a positive control. The percentage membrane stabilization (protection from lysis) was measured as:

$$\%\ \boldsymbol{of\ Stabilization} = \frac{\boldsymbol{A\ Control - A\ Sample}}{\boldsymbol{Acontrol}} \boldsymbol{X100}$$

Statistical Analysis

Experiments were performed in triplicate, with results expressed as mean ± SD. Statistical analysis was conducted using Origin software. Group differences were assessed by one-way ANOVA followed by Tukey's post hoc test. Significance was set at $p < 0.05$.

RESULTS

Separation of Astaxanthin from freshwater algae *Haematococcus pluvialis*

The extraction procedure using acetone successfully yielded a concentrated astaxanthin-rich product from *Haematococcus pluvialis* (Figure 1 a). Visual observation confirmed a deep red coloration in the acetone extract, which faded progressively in the biomass pellet after each extraction cycle, suggesting exhaustive pigment recovery (Figure 1 b). The rotary evaporation of the pooled extracts at 40 °C yielded 36.8 mg of reddish crude extract from 10 g of dried biomass.

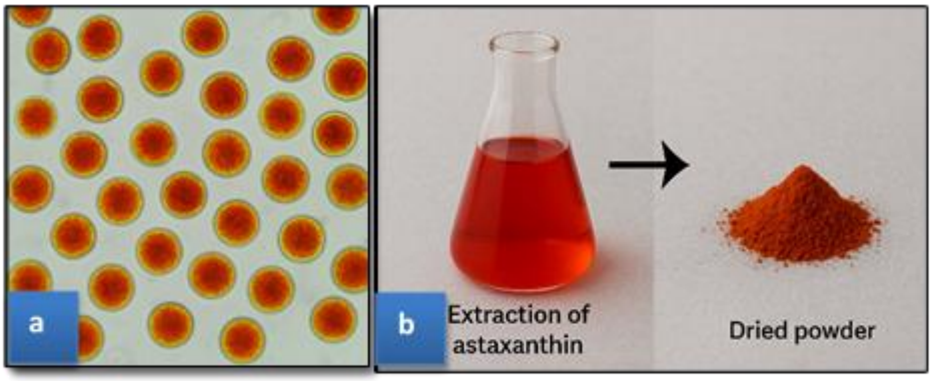

Figure 1: Extraction of Astaxanthin from Microalgae: (a) Microscopic view of astaxanthin-rich microalgal cells, (b) Solvent extract and resulting dried astaxanthin powder.

UV–Visible Spectroscopic Analysis

UV-Visible spectroscopic analysis of the green-synthesized Zinc oxide nanoparticles (ZnO NPs) integrated with astaxanthin from *Haematococcus pluvialis* showed a distinct absorption peak at 360 nm, confirming the formation of ZnO NPs (Figure 2 a). This peak matches to the characteristic band-gap transition of ZnO, indicating successful synthesis.

Fourier Transform Infrared (FTIR) Spectroscopy

The FTIR spectrum of green-synthesized ZnO NPs integrated with astaxanthin from *Haematococcus pluvialis* showed a wide peak at 3398 cm^{-1} matches to O–H stretching, while 1661 cm^{-1} indicates C=O stretching from carbonyl groups. Peaks at 1521 and 1375 cm^{-1} are corresponding to C=C and C–H bending, respectively. The band at 1001 cm^{-1} suggests C–O stretching, while 832 and 704 cm^{-1} are due to aromatic C–H bending. The peak at 581 cm^{-1} confirms Zn–O bond formation, indicating successful synthesis and capping of ZnO NPs by astaxanthin (Figure 2 b).

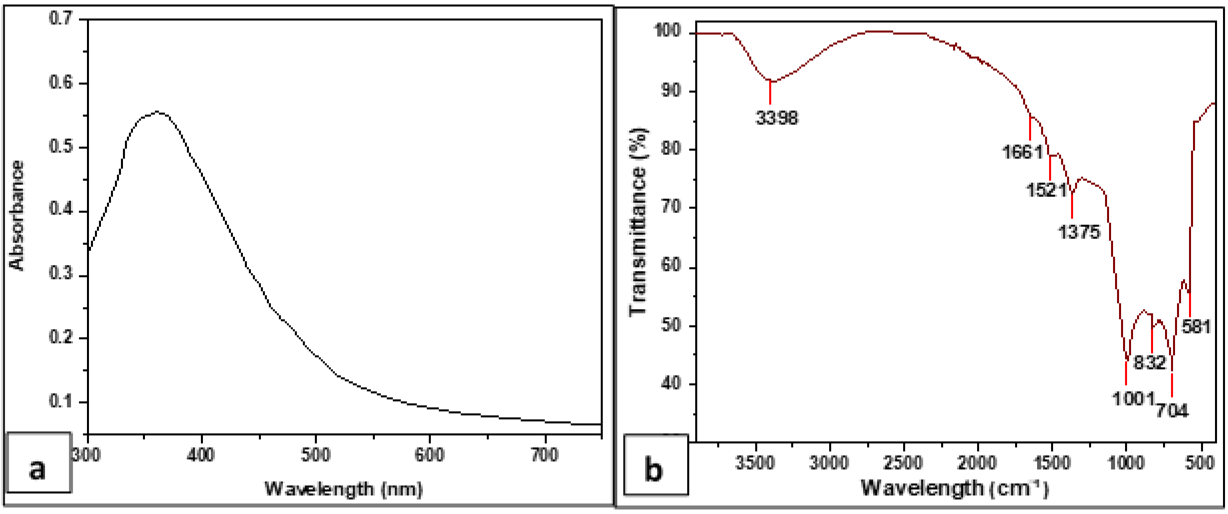

Figure 2: (a) UV-Visible and (b) FTIR spectral analysis of green synthesis of ZnO NPs integrated with astaxanthin from *Haematococcus pluvialis*

Dynamic Light Scattering (DLS) and Zeta Potential

DLS analysis indicated a narrow particle size distribution with an average hydrodynamic diameter of approximately 85–110 nm, which was slightly higher than the XRD-based crystallite size due to the hydration shell in aqueous suspension (Figure 3 A). Zeta potential measurements showed a surface charge of –27.5 mV, suggesting that the nanoparticles were moderately stable due to electrostatic repulsion among particles (Figure 3 B). The negative potential further indicated the successful incorporation of astaxanthin, which contributed to surface functionalization and dispersion stability.

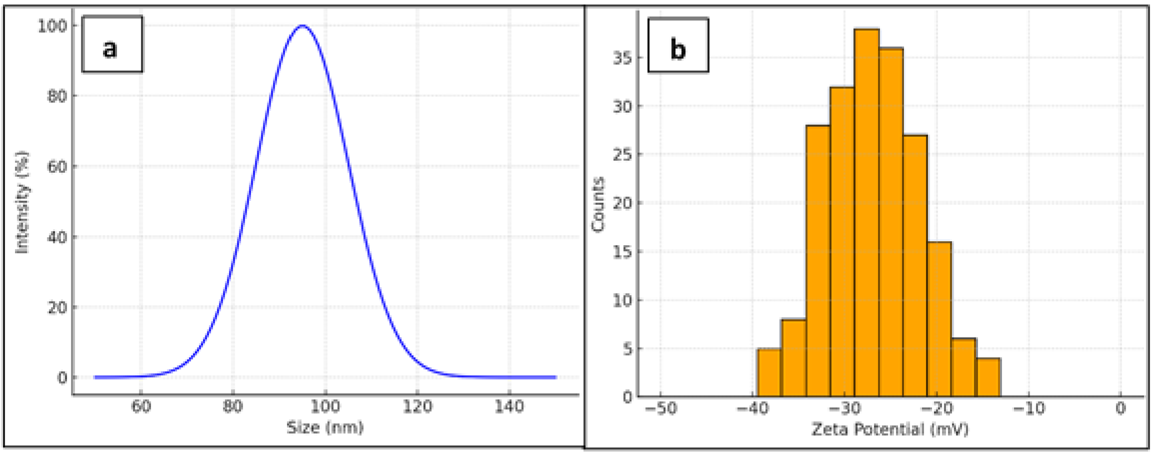

Figure 3: DLS and Zeta potential spectral analysis (A & B) of green synthesis of ZnO NPs integrated with astaxanthin from *Haematococcus pluvialis*

Scanning Electron Microscopic (SEM) Analysis

SEM images provided insight into the surface morphology and topography of ZnO-astaxanthin NPs. The particles appeared predominantly spherical with slight agglomeration, typical of biosynthesized nanoparticles. The average size observed under SEM ranged between 50–80 nm, corroborating DLS result (Figure 4). The relatively smooth surface and uniform shape further confirmed the role of astaxanthin in controlling nanoparticle morphology and preventing excessive aggregation

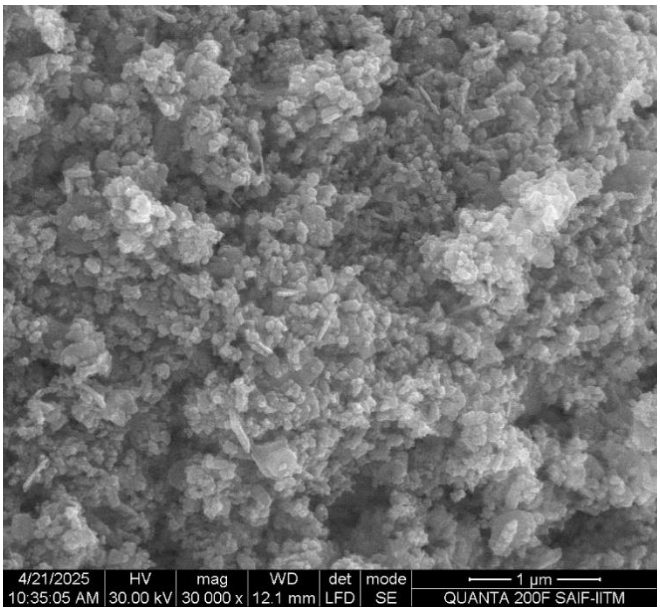

Figure 4: SEM analysis of green synthesis of ZnO NPs integrated with astaxanthin from *Haematococcus pluvialis*

Antioxidant Activities

The antioxidant prospective of the sample was assessed using three distinct in vitro assays: DPPH radical scavenging, hydrogen peroxide (H_2O_2) scavenging, and nitric oxide (NO) radical inhibition. Each assay was performed using varying concentrations of the test compound (10, 20, 40, 60, 80, and 100 µg/mL), with ascorbic acid serving as the positive control. The scavenging effect was measured as percentage inhibition.

DPPH Radical Scavenging Activity

The DPPH assay verified a steady increase in DPPH scavenging with increasing concentration of the test compound. At 10 µg/mL, the sample showed 13.7% inhibition, which rose steadily to 76.45% at 100 µg/mL. The standard, ascorbic acid, exhibited 82.41% inhibition. These results suggest that the test compound has considerable DPPH radical scavenging in a dose-dependent manner, approaching the efficacy of the standard antioxidant (Figure. 5).

Hydrogen Peroxide (H_2O_2) Scavenging Activity

The H_2O_2 scavenging assay revealed that the test compound efficiently reduced hydrogen peroxide radicals. The percentage inhibition increased from 17.3% at 10 µg/mL to 77.97% at 100 µg/mL. In comparison, ascorbic acid showed a slightly higher inhibition of 81.62%, indicating the compound's potent antioxidant action, albeit slightly lower than the reference standard (Figure 5).

Nitric Oxide (NO) Radical Inhibition Assay

In the NO radical scavenging assay, the compound displayed strong inhibitory activity. The inhibition percentage began at 15.9% for 10 µg/mL and reached 80.07% at 100 µg/mL. The standard ascorbic acid showed a maximum inhibition of 89.33%. This finding suggests that the test compound effectively neutralizes nitric oxide radicals, though slightly less efficient than the standard (Figure 5).

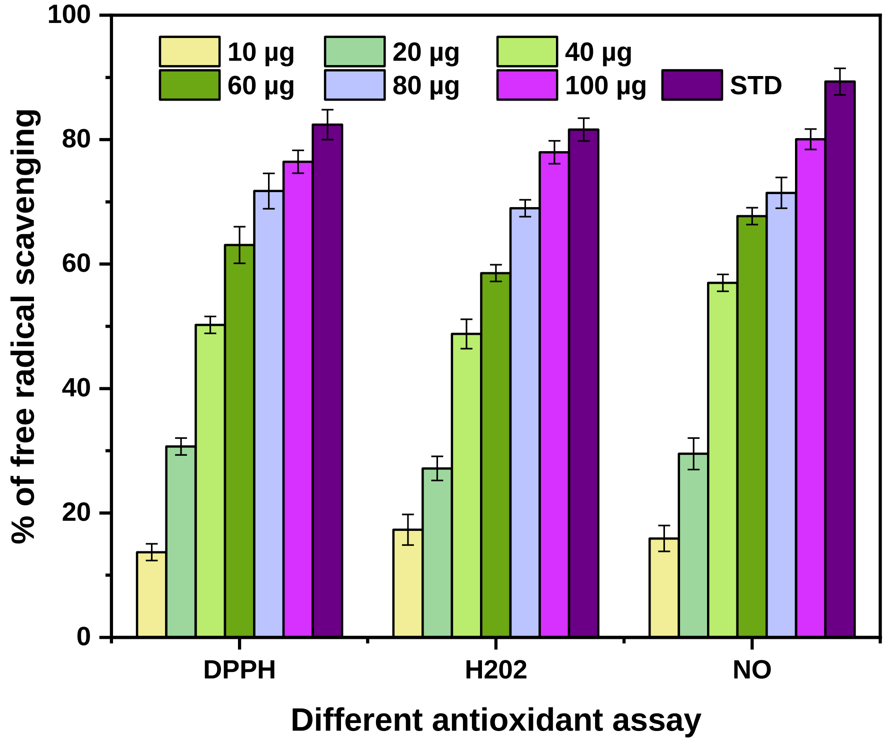

Figure 5: Antioxidant activities of green synthesis of ZnO NPs integrated with astaxanthin from *Haematococcus pluvialis*

Anti-inflammatory assay

The anti-inflammatory effect of the Bio-synthesized ZnO-astaxanthin nanoparticles was assessed by means of *in vitro* protein denaturation inhibition assay and membrane stabilization assay, which simulate inflammatory conditions by evaluating the inhibition of albumin denaturation and erythrocyte membrane lysis, respectively.

Protein Denaturation Inhibition Assay

The ZnO-astaxanthin nanoparticles demonstrated protein denaturation inhibition in a concentration-dependent manner, with values ranging from 28.4% at 10 µg/mL to 81.3% at 100 µg/mL. In contrast, the conventional anti-inflammatory agent diclofenac sodium demonstrated inhibition levels ranging from 34.5% to 91.2% across the corresponding concentration range (Figure 6a). At higher concentrations (80–100 µg/mL), the nanoparticles showed substantial inhibitory activity, closely approaching that of the standard, suggesting effective prevention of heat-induced protein denaturation.

Human Red Blood Cell (HRBC) Membrane Stabilization Assay

Similarly, the nanoparticles exhibited significant membrane stabilization activity, with protection increasing from 25.3% at 10 µg/mL to 79.7% at 100 µg/mL. Diclofenac sodium, employed as the standard reference drug, exhibited membrane stabilization effects between 31.6% and 89.5% across the tested concentration range (Figure 6b). The data indicated that ZnO-astaxanthin nanoparticles were capable of stabilizing erythrocyte membranes under hypotonic stress, thereby mimicking the lysosomal membrane stability associated with anti-inflammatory effects.

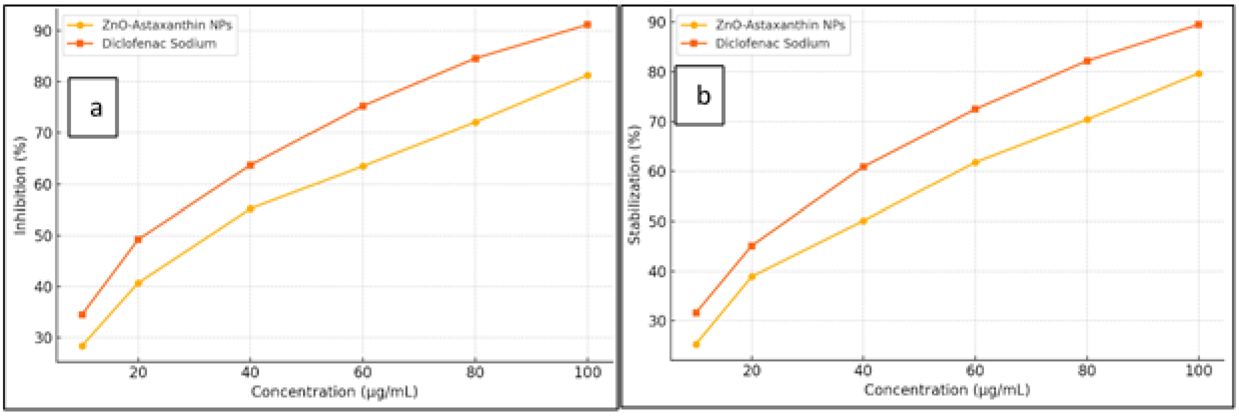

Figure 6: Comparative anti-inflammatory activity of ZnO-Astaxanthin NPs and diclofenac sodium assessed by (a) protein denaturation inhibition and (b) HRBC membrane stabilization assay.

DISCUSSION

The current study highlights the successful green synthesis, evaluation of physicochemical property, and bioactivity evaluation of zinc oxide nanoparticles (ZnO NPs) functionalized with astaxanthin extracted from *Haematococcus pluvialis.* Astaxanthin, a potent xanthophyll carotenoid, is well acknowledged for its exceptional antioxidant and anti-inflammatory properties, which have been effectively harnessed here for nanoparticle synthesis and biofunctionalization [15].

The extraction of astaxanthin using acetone yielded a deep red pigment characteristic of this carotenoid, aligning with previous studies demonstrating acetone's efficiency in carotenoid recovery from *H. pluvialis* due to its high polarity and solvation capacity [16]. The UV–Vis spectroscopic analysis of ZnO-astaxanthin nanoparticles showed a distinct absorption peak at 360 nm, which is consistent with the intrinsic bandgap of ZnO NPs and confirms successful nanoparticle formation[17]. FTIR analysis further supported the functionalization of ZnO with astaxanthin, as evidenced by characteristic peaks consistent to hydroxyl (O–H), carbonyl (C=O), and aromatic bonds, along with a Zn–O stretch around 581 cm^{-1}. This implies that astaxanthin act both as a reactant and stabilizing agent, a feature commonly observed in green synthesis approaches employing phytochemicals[18].

DLS and zeta potential analyses confirmed the formation of moderately stable nanoparticles with a size distribution in the range of 85–110 nm and a surface charge of –27.5 mV. The negative zeta potential suggests electrostatic stabilization of the nanoparticle dispersion and supports the successful capping by astaxanthin molecules [19]. SEM imaging revealed spherical morphology with minimal aggregation, corroborating other reports where bioactive compounds influence nanoparticle morphology and dispersibility [20].

The ZnO-astaxanthin nanoparticles exhibited strong, concentration-dependent antioxidant activity in all three assays: DPPH, H_2O_2, and NO scavenging. The radical inhibition values approached those of the standard ascorbic acid, particularly at higher concentrations[21]. The witnessed activity may be due to the synergistic effect of the inherent antioxidant properties of both ZnO and astaxanthin [22]. ZnO nanoparticles are known to exhibit ROS-scavenging abilities, while astaxanthin, due to its extended conjugated polyene chain, can efficiently quench free radicals [23].

These results are consistent with the literature, where astaxanthin-loaded nanoparticles have revealed boosted antioxidant activity compared to free astaxanthin, likely due to improved solubility, stability, and cellular uptake. Such antioxidant potential underscores their promise in biomedical applications, particularly in mitigating oxidative stress-associated disorders[24].

In vitro anti-inflammatory assays demonstrated that ZnO-astaxanthin nanoparticles could significantly inhibit protein denaturation and stabilize HRBC membranes in a dose-dependent manner. Protein denaturation is a hallmark of inflammation, and its inhibition is a key indicator of anti-inflammatory efficacy [25]. The nanoparticles displayed inhibition percentages comparable to the reference drug diclofenac sodium, indicating that the nanoconjugate formulation retained, and possibly enhanced, the anti-inflammatory potential of astaxanthin. The HRBC membrane stabilization assay simulates the lysosomal membrane, where stabilization reflects the potential to prevent the release of inflammatory mediators[26]. The nanoparticles exhibited substantial membrane protection, further confirming their anti-inflammatory capability. These outcomes are in line with prior reports where astaxanthin and ZnO nanoparticles individually exhibited anti-inflammatory activity through inhibition of inflammatory cytokines and protection of cell membranes [27].

Notably, the improved bioactivity observed in this study may be attributed to the nano-formulated delivery system, which potentially enhanced the bioavailability and stability of astaxanthin, known for its poor water solubility and susceptibility to degradation[28].

Encapsulating bioactive like astaxanthin into nanocarriers is a well-documented strategy for overcoming such limitations and enhancing therapeutic efficacy.

CONCLUSION

The current study effectively validated the green synthesis of zinc oxide nanoparticles (ZnO NPs) using astaxanthin extracted from *Haematococcus pluvialis*. The extractive process yielded a richly pigmented astaxanthin extract, and subsequent characterization confirmed the effective synthesis and capping of ZnO NPs by astaxanthin. Spectroscopic and microscopic analyses, including UV–Vis, FTIR, DLS, zeta potential, and SEM, validated the formation of stable, spherical nanoparticles with appropriate size and surface charge. The ZnO-astaxanthin nanoparticles exhibited potent antioxidant activity across DPPH, H_2O_2, and nitric oxide scavenging assays, with inhibition levels comparable to the standard antioxidant, ascorbic acid. Furthermore, the nanoparticles showed notable anti-inflammatory activity as evidenced by their concentration-dependent efficacy in protein denaturation inhibition and stabilizing erythrocyte membranes, approaching the performance of the standard drug diclofenac sodium. These outcomes highlight the promising therapeutic potential of ZnO-astaxanthin nanoparticles as effective bioactive agents with both antioxidant and anti-inflammatory properties. This eco-friendly synthesis approach provides a sustainable platform for developing nanomedicine formulations derived from natural biomolecules.

ACKNOWLEDGEMENT

The authors gratefully acknowledge the support provided by Saveetha Medical College and Hospital, Saveetha Institute of Medical and Technical Sciences (SIMATS), Thandalam, Chennai–602105, Tamil Nadu, India, for facilitating this research work and providing the necessary infrastructure and resources.

REFERENCES

1. Malik, S., Muhammad, K., and Y. Waheed. "Emerging Applications of Nanotechnology in Healthcare and Medicine." *Molecules*, vol. 28, 2023, article 6624. MDPI, https://doi.org/10.3390/molecules28186624.
2. Krishna, S. B. N., Jakmunee, J., Mishra, Y. K., and J. Prakash. "ZnO Based 0–3D Diverse Nano-Architectures, Films and Coatings for Biomedical Applications." *Journal of Materials Chemistry B*, vol. 12, 2024, pp. 2950–2984. Royal Society of Chemistry, https://doi.org/10.1039/D4TB00184B.
3. Kirubakaran, D., Wahid, J. B. A., Karmegam, N., Jeevika, R., Sellapillai, L., Rajkumar, M., and K. J. SenthilKumar. "A Comprehensive Review on the Green Synthesis of Nanoparticles: Advancements in Biomedical and Environmental Applications." *Biomedical Materials and Devices*, 2025, https://doi.org/10.1007/s44174-025-00295-4.
4. Varshan, G. S. A., and S. K. R. Namasivayam. "A Green Chemistry Principle for the Biotransformation of Fungal Biomass Derived Chitosan into Versatile Nanoscale Materials with High Biocompatibility and Potential Biological Activities—A Review." *Bionanoscience*, vol. 14, 2024, pp. 4145–4166. Springer, https://doi.org/10.1007/s12668-024-01564-0.
5. Ahmad Kamal, A. H., et al. "Genetically Engineered Microalgae for Enhanced Bioactive Compounds." *Discoveries and Applications in Science*, vol. 6, 2024, article 482. Springer, https://doi.org/10.1007/s42452-024-06116-5.
6. Tambat, V. S., et al. "Advancing Sustainable Astaxanthin-Lipid Biorefineries: Robust Two-Stage Phytohormone-Driven Bioprocess in *Chromochloris zofingiensis*." *Bioresource Technology Reports*, vol. 29, 2025, article 102022. Elsevier, https://doi.org/10.1016/j.biteb.2025.102022.
7. Aneesh, P. A., et al. "Bioactivities of Astaxanthin from Natural Sources, Augmenting Its Biomedical Potential: A Review." *Trends in Food Science & Technology*, vol. 125, 2022, pp. 81–90. Elsevier, https://doi.org/10.1016/j.tifs.2022.05.004.
8. Huang, L., et al. "Dietary Fatty Acid-Mediated Protein Encapsulation Simultaneously Improving the Water-Solubility, Storage Stability, and Oral Absorption of Astaxanthin." *Food Hydrocolloids*, vol. 123, 2022, article 107152. Elsevier, https://doi.org/10.1016/j.foodhyd.2021.107152
9. Pitacco, W., et al. "Extraction of Astaxanthin from *Haematococcus pluvialis* with Hydrophobic Deep Eutectic Solvents Based on Oleic Acid." *Food Chemistry*, vol. 379, 2022, article 132156. Elsevier, https://doi.org/10.1016/j.foodchem.2022.132156.
10. Chandramohan, S., Francis, A. P., Pajaniradje, S., and R. Rajagopalan. "Green and Chemical Synthesized Zinc Oxide Nanoparticles: Evaluation of Their Anti-Proliferative Activity against Breast Cancer Cell Line—An *In Vitro* and *In Silico* Approach." *Particle Science and Technology*, vol. 42, 2024, pp. 1155–1177. Taylor & Francis, https://doi.org/10.1080/02726351.2024.2364859.
11. Kannan, K., and P. Sivaperumal. "Antibacterial Efficacy against Urinary Tract Infection (UTI) Pathogens and Free Radical Scavenging Potential of Marine Algae *Sargassum wightii* Mediated Copper Nanoparticles." *Bionanoscience*, vol. 15, 2025, p. 371. Springer, https://doi.org/10.1007/s12668-025-02007-0.

12. Marvi, P. K., et al. "*Prunella vulgaris*-Phytosynthesized Platinum Nanoparticles: Insights into Nanozymatic Activity for H_2O_2 and Glutamate Detection and Antioxidant Capacity." *Talanta*, vol. 274, 2024, article 125998. Elsevier, https://doi.org/10.1016/j.talanta.2024.125998.
13. Thida, M., Aung, H. M., Wai, N. P., and T. S. Moe. "*In Vitro* Evaluation of Antioxidant, Antiglycation and Anti-Protein Denaturation Potentials of Indigenous Myanmar Medicinal Plant Extracts." *Journal of Herbs, Spices & Medicinal Plants*, vol. 30, 2024, pp. 278–291. Taylor & Francis, https://doi.org/10.1080/10496475.2024.2353140.
14. Sangeeta, M. K., et al. "*In Vitro* Evaluation of *Talaromyces islandicus* Mediated Zinc Oxide Nanoparticles for Antibacterial, Anti-Inflammatory, Bio-Pesticidal and Seed Growth Promoting Activities." *Waste and Biomass Valorization*, vol. 15, 2024, pp. 1901–1915. Springer, https://doi.org/10.1007/s12649-023-02386-z.
15. Abdelazim, K., et al. "Production and Therapeutic Use of Astaxanthin in the Nanotechnology Era." *Pharmacological Reports*, vol. 75, 2023, pp. 771–790. Springer, https://doi.org/10.1007/s43440-023-00488-y.
16. Jiang, Y., et al. "Extraction and Synthesis of Typical Carotenoids: Lycopene, β-Carotene, and Astaxanthin." *Molecules*, vol. 29, 2024, article 4549. MDPI, https://doi.org/10.3390/molecules29194549.
17. Singh, S., et al. "Exploring ZnO Nanoparticles: UV–Visible Analysis and Different Size Estimation Methods." *Optical Materials*, vol. 152, 2024, article 115422. Elsevier, https://doi.org/10.1016/j.optmat.2024.115422.
18. El-Belely, E. F., et al. "Green Synthesis of Zinc Oxide Nanoparticles (ZnO-NPs) Using *Arthrospira platensis* (Class: Cyanophyceae) and Evaluation of Their Biomedical Activities." *Nanomaterials*, vol. 11, 2021, article 95. MDPI, https://doi.org/10.3390/nano11010095.
19. Sridhar, K., Inbaraj, B. S., and B.-H. Chen. "Recent Advances on Nanoparticle Based Strategies for Improving Carotenoid Stability and Biological Activity." *Antioxidants*, vol. 10, 2021, article 713. MDPI, https://doi.org/10.3390/antiox10050713.
20. Sezen, G., and R. Aktan. "Green Synthesis of Zinc Oxide Particles Using *Cladophora glomerata* L. (Kütz) Extract: Comparative Study of Crystal Structure, Surface Chemistry, and Antimicrobial Efficacy with Different Zinc Precursors." *Processes*, vol. 13, 2025, article 2350. MDPI, https://doi.org/10.3390/pr13082350.
21. Azeem, M., et al. "Assessing Anticancer, Antidiabetic, and Antioxidant Capacities in Green-Synthesized Zinc Oxide Nanoparticles and Solvent-Based Plant Extracts." *Heliyon*, vol. 10, 2024, e34073. Elsevier, https://doi.org/10.1016/j.heliyon.2024.e34073.
22. Nasri, N., et al. "Enhancement of Astaxanthin Production in *Haematococcus pluvialis* Using Zinc Oxide Nanoparticles." *Journal of Biotechnology*, vol. 342, 2021, pp. 72–78. Elsevier, https://doi.org/10.1016/j.jbiotec.2021.10.004.
23. Gu, J., et al. "An Enhanced Antioxidant Strategy of Astaxanthin Encapsulated in ROS-Responsive Nanoparticles for Combating Cisplatin-Induced Ototoxicity." *Journal of Nanobiotechnology*, vol. 20, 2022, article 268. Springer, https://doi.org/10.1186/s12951-022-01485-8.
24. Hien, H. T. M., et al. "Astaxanthin-Loaded Nanoparticles Enhance Its Cell Uptake, Antioxidant and Hypolipidemic Activities in Multiple Cell Lines." *Journal of Drug Delivery Science and Technology*, vol. 80, 2023, article 104133. Elsevier, https://doi.org/10.1016/j.jddst.2022.104133.
25. Rehman, H., et al. "*Delphinium uncinatum* Mediated Biosynthesis of Zinc Oxide Nanoparticles and *In Vitro* Evaluation of Their Antioxidant, Cytotoxic, Antimicrobial, Anti-Diabetic, Anti-Inflammatory, and Anti-Aging Activities." *Saudi Journal of Biological Sciences*, vol. 30, 2023, article 103485. Elsevier, https://doi.org/10.1016/j.sjbs.2022.103485.
26. Qasim, S., et al. "Rosuvastatin Attenuates Rheumatoid Arthritis-Associated Manifestations via Modulation of the Pro- and Anti-Inflammatory Cytokine Network: A Combination of *In Vitro* and *In Vivo* Studies." *ACS Omega*, vol. 6, 2021, pp. 2074–2084. American Chemical Society, https://doi.org/10.1021/acsomega.0c05054.
27. Mawed, S. A., et al. "*Dunaliella salina* Microalga Restores the Metabolic Equilibrium and Ameliorates the Hepatic Inflammatory Response Induced by Zinc Oxide Nanoparticles (ZnO-NPs) in Male Zebrafish." *Biology*, vol. 11, 2022, article 1447. MDPI, https://doi.org/10.3390/biology11101447.
28. Bharti, A., Hooda, V., Jain, U., and N. Chauhan. "Astaxanthin: A Nature's Versatile Compound Utilized for Diverse Applications and Its Therapeutic Effects." *3 Biotech*, vol. 15, 2025, article 88. Springer, https://doi.org/10.1007/s13205-025-04241-5.